



Science Arts & Métiers (SAM)

is an open access repository that collects the work of Arts et Métiers Institute of Technology researchers and makes it freely available over the web where possible.

This is an author-deposited version published in: <https://sam.ensam.eu>
Handle ID: <http://hdl.handle.net/10985/23241>

To cite this version :

Xi YANG, Adil EL BAROUDI, Jean Yves LE POMMELLEEC - Free vibration investigation of submerged thin circular plate - International Journal of Applied Mechanics - 2020

Any correspondence concerning this service should be sent to the repository

Administrator : scienceouverte@ensam.eu



Free vibration investigation of submerged thin circular plate

Xi YANG and Adil EL BAROUDI and Jean Yves LE POMMELLEC

LAMPA, Arts et Metiers Institute of Technology

2 Bd du Ronceray

49035 Angers Cedex 1, France

adil.elbaroudi@ensam.eu

11 Free vibration of coupled system including clamped-free thin circular plate with hole
12 submerged in three dimensional cylindrical container filled with inviscid, irrotational
13 and compressible fluid is investigated in the present work. Numerical approach based on
14 the finite element method (FEM) is performed using the Comsol Multiphysics software,
15 in order to analyze qualitatively the vibration characteristics of the plate. Plate modeling
16 is based on Kirchhoff-Love plate theory. Velocity potential is deployed to describe the
17 fluid motion since the small oscillations induced by the plate vibration is considered.
18 Bernoulli's equation together with potential theory are applied to get the fluid pressure
19 on the free surface of the plate. To prove the reliability of the present numerical solution, a
20 comparison is made with the results in the literature, which shows a very good agreement.
21 Then, different parameters effect including fluid density, fluid height, free surface wave,
22 hole radius and hole eccentricity on the natural frequencies of the coupled system is
23 discussed in detail. Some three-dimensional mode shapes of the submerged plate are
24 illustrated. Furthermore, the obtain results can serve as benchmark solutions for the
25 vibration control, parameter identification and damage detection of plate.

Keywords: Fluid-structure interaction; Thin circular plate; Finite element procedure.

1. Introduction

28 Fluid-structure interaction occurs especially when an elastic structure vibrates in
29 presence of a fluid domain. By virtue of inertia increase due to the fluid motion
30 generated by vibrating structure, the natural frequencies are significantly lower
31 than those in vacuum. This behavior has been justified by the concept of the gradual
32 increase in the added mass. This study is particularly concerned with free vibration
33 analysis of circular plate with hole submerged in fluid.

Circular plates with or without hole in contact or not with fluid are widely
used in many branches of engineering, e.g. liquid storage tanks, offshore naval or
marine structures, solar plates, nuclear reactor internal components, micro pumps
and circular disk of butterfly valves. Also, baffles and perforated plates are efficient
for reducing resonant sloshing in moving tank containing liquid [Jin *et al.*, 2014; Xue
et al., 2017; Yu *et al.*, 2019; Ghalandari *et al.*, 2019]. On the one hand, in vacuum, the
existence of hole in a circular plate can significantly affect its vibrational response.

41 The knowledge and understanding of the associated effects is useful to the design of
42 structures and vibration control. Therefore, studying and analyzing the vibrational
43 behavior of circular plate with hole, is of high importance. A number of research
44 works have been conducted on the vibration analysis of such structures based on
45 analytical, experimental and numerical methods, such as the FEM, energy approach
46 and mode subtraction approach. Excellent reference sources available may be found
47 in the literature [Khurasia and Rawtani, 1978; Leissa and Narita, 1980; Nagaya and
48 Poltorak, 1989; Vega *et al.*, 1998; Chen *et al.*, 2006; Lee *et al.*, 2007; Jhung and
49 Jeong, 2015].

50 On the other hand, several researchers have investigated the vibration of plates in
51 contact with a fluid and there have been many excellent experimental and theoretical
52 research papers [Kwak, 1991; Bauer, 1995; Amabili and Kwak, 1996; Ergin and
53 Ugurlu, 2003; Jhung *et al.*, 2009; Askari *et al.*, 2013; Soltani and Reddy, 2015; Cho
54 *et al.*, 2015; Gascon-Pérez and Garcia-Fodega, 2015]. Obviously, the presence of the
55 fluid around the plate causes an increase in the kinetic energy, and consequently,
56 the natural frequencies of plate coupled with fluid strongly decrease compared to
57 those obtained in vacuum. Certainly, this will significantly affect the coupled system
58 performance under dynamic loading. However, the vibration analysis of a circular
59 plate with a hole submerged in fluid taking into account both the free surface
60 wave and eccentricity of the hole is missing in the literature. A good understanding
61 of the dynamic interactions between the plate and fluid is necessary. Due to the
62 dynamic nature of the system, the boundaries and the fluid-structure interaction
63 forces between the plate and the fluid do not remain constant. Therefore, the need
64 for fluid-structure interaction modelling seems inevitable for the structure and fluid
65 [Gascon-Pérez, 2015; Mnassri and El Baroudi, 2017; Bahaadini and Saidi, 2018;
66 Bahaadini *et al.*, 2018a,b; Saidi *et al.*, 2019].

67 The aim of the present research is to investigate numerically the vibration analy-
68 sis of circular plate with hole submerged in fluid. A three-dimensional finite element
69 model is constructed using Comsol Multiphysics software and the natural frequen-
70 cies and corresponding mode shapes are obtained. The results show a very good
71 agreement with those in literature in some particular cases. Moreover, the effect of
72 different parameters including fluid density, fluid height, free surface wave, hole size
73 and hole eccentricity on the vibration characteristics are examined.

74 **2. Mathematical formulation for a plate submerged in fluid**

75 A thin circular plate with hole submerged in a fluid-filled cylindrical rigid container,
76 where a , b and h ($\ll a$) represent the outer radius, inner radius and thickness of
77 the plate, respectively (see Fig. 1), is considered. The cylindrical container radius
78 is R and the fluid depth is H . The fluid domain is divided into two regions : an
79 upper fluid region (its depth is represented by H_u) and lower fluid region (its depth is
80 represented by H_l). The present work is based on the following assumptions : (i) the
81 fluid is assumed to be inviscid, irrotational, and compressible, and the amplitude of

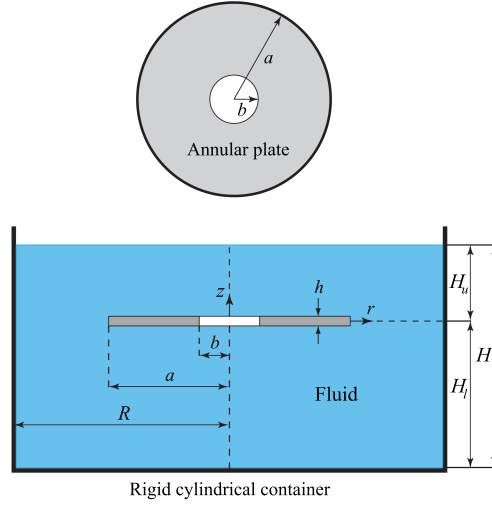


Fig. 1. Circular plate with hole submerged in fluid.

82 fluid motion is small in comparison with the model dimensions; (ii) the plate is made
 83 to be linearly elastic, homogeneous and isotropic; and (iii) the shear deformation
 84 and rotary inertia on the dynamics of plate are negligible. For the plate, the outer
 85 and inner boundaries are subject to the clamped and free boundary conditions,
 86 respectively. The equation of motion for the plate transverse displacement, w is

$$D\nabla^4 w + \rho_s h \partial_{tt} w = p \quad (1)$$

87 where D , ρ_s , h are respectively the bending rigidity, density, thickness and p is the
 88 hydrodynamic pressure on the surface of the plate. The bending rigidity of the plate
 89 is expressed as $D = Eh^3 / (12(1 - \nu^2))$ where E is Young's modulus and ν is the
 90 Poisson's ratio. Since the small fluid oscillations induced by the plate vibration is
 91 considered, the fluid motion can be described using the velocity potential function
 92 Φ which should satisfy the wave equation [Kinsler *et al.*, 1999]

$$B\nabla^2 \Phi - \rho_f \partial_{tt} \Phi = 0 \quad (2)$$

93 where $B = \rho_f c_f^2$ is the fluid bulk modulus of elasticity, ρ_f is the fluid density and
 94 c_f is the sound wave speed. The fluid bulk modulus of elasticity is used to take
 95 into account the fluid compressibility. The fluid velocity is related to the potential
 96 function by following expression

$$\mathbf{v} = \nabla \Phi \quad (3)$$

97 The pressure given in Eq. (1) is related to velocity potential function by

$$p = -\rho_f \partial_t \Phi \quad (4)$$

98 **2.1. Plate-fluid boundary conditions**

99 To study the influence of fluid density on the natural frequencies of plate, or the
100 plate effect on the free surface, boundary conditions are formulated as : (i) In the
101 case of impermeable boundaries, which means that the fluid velocity in the normal
102 direction to the surface is equal to zero, the boundary condition is expressed as

$$\nabla\Phi \cdot \mathbf{n} = 0 \quad (5)$$

103 where \mathbf{n} is the normal vector at the fluid boundary. (ii) As the velocity potential is
104 associated with the plate movement only (when the surface wave effect is neglected),
105 the zero pressure condition is assumed at the free fluid surface, which means

$$p = -\rho_f \partial_t \Phi = 0 \quad (6)$$

106 (iii) When the free surface wave condition (or sloshing condition) is assumed, ne-
107 glecting surface tension the sloshing condition is obtained from kinetic and kine-
108 matic conditions, yields the following relation

$$g\nabla\Phi \cdot \mathbf{n} = -\partial_{tt}\Phi \quad (7)$$

109 where g represents the acceleration due to gravity. (iv) During the interaction be-
110 tween the plate and fluid, the fluid particle and the plate move together in the
111 normal direction of the boundary, and the interface boundary condition can be
112 written as

$$\nabla\Phi \cdot \mathbf{n} = \partial_t w \quad (8)$$

113 **2.2. Numerical solution: Variational Formulation**

In this section we construct the variational formulation of the problem defined by Eqs. (1) and (2) in terms of w and Φ . The used numerical formulations include displacement formulation, potential formulation, pressure formulation and combination of some of them. Numerical solution based on FEM is used to extract frequencies and modal shapes. To compute the vibration modes of a fluid alone, the fluid is typically described either by pressure or by displacement potential variables. When the fluid is coupled with a solid, [Morand and Ohayon, 1979] introduce an alternative procedure which consists in using pressure and displacement potential simultaneously. In this section we summarize their approach and further details can be found in their book [Morand and Ohayon, 1995]. Therefore, to obtain a variational formulation for submerged plate, Eqs. (1) and (2) are multiplied by arbitrary test functions $(\bar{w}, \bar{\Phi})$ and integrating over the domains Ω_s and Ω_f (plate and fluid) using Green's formula and taking into account the boundary conditions yields

$$\int_{\Omega_s} D\nabla^2 w \cdot \nabla^2 \bar{w} d\Omega_s - \omega^2 \int_{\Omega_s} \rho_s h w \bar{w} d\Omega_s + j\omega \int_{\Omega_s} \rho_f \Phi \bar{w} d\Omega_s = 0 \quad (9)$$

$$\int_{\Omega_f} \rho_f \nabla\Phi \cdot \nabla\bar{\Phi} d\Omega_f - \omega^2 \int_{\Omega_f} \frac{\rho_f}{c_f^2} \Phi \bar{\Phi} d\Omega_f - j\omega \int_{\partial\Omega_f} \rho_f w \bar{\Phi} d\Gamma_f = 0 \quad (10)$$

Applying standard Galerkin discretization method which consists in constructing an approximate solution of Eqs. (9) and (10), we have

$$\left\{ \begin{pmatrix} \mathbf{K}_w & \mathbf{0} \\ \mathbf{0} & \mathbf{K}_\Phi \end{pmatrix} - \omega^2 \begin{pmatrix} \mathbf{M}_w & \mathbf{0} \\ \mathbf{0} & \mathbf{M}_\Phi \end{pmatrix} + j\omega \begin{pmatrix} \mathbf{0} & \mathbf{C}_w \\ -\mathbf{C}_\Phi & \mathbf{0} \end{pmatrix} \right\} \begin{Bmatrix} \mathbf{W} \\ \mathbf{\Phi} \end{Bmatrix} = \begin{Bmatrix} \mathbf{0} \\ \mathbf{0} \end{Bmatrix} \quad (11)$$

where \mathbf{W} and $\mathbf{\Phi}$ are the vectors of nodal values for w and Φ , respectively, and the matrices in Eq. (11) are defined by

$$\begin{aligned} \int_{\Omega_s} D \nabla^2 w \cdot \nabla^2 \bar{w} d\Omega_s &= \bar{\mathbf{W}}^T \mathbf{K}_w \mathbf{W}, \quad \int_{\Omega_s} \rho_s h w \bar{w} d\Omega_s = \bar{\mathbf{W}}^T \mathbf{M}_w \mathbf{W} \\ \int_{\Omega_s} \rho_f \Phi \bar{w} d\Omega_s &= \bar{\mathbf{W}}^T \mathbf{C}_w \mathbf{\Phi}, \quad \int_{\Omega_f} \rho_f \nabla \Phi \cdot \nabla \bar{\Phi} d\Omega_f = \bar{\mathbf{\Phi}}^T \mathbf{K}_\Phi \mathbf{\Phi} \\ \int_{\Omega_f} \frac{\rho_f}{c_f^2} \Phi \bar{\Phi} d\Omega_f &= \bar{\mathbf{\Phi}}^T \mathbf{M}_\Phi \mathbf{\Phi}, \quad \int_{\partial\Omega_f} \rho_f w \bar{\Phi} d\Gamma_f = \bar{\mathbf{\Phi}}^T \mathbf{C}_\Phi \mathbf{W} \end{aligned}$$

114 where $\bar{\mathbf{W}}$ and $\bar{\mathbf{\Phi}}$ are the vectors of nodal values for \bar{w} and $\bar{\Phi}$, respectively. In order to determine natural frequencies of free vibration of submerged plate, Comsol
 115 Multiphysics code is used [Comsol, 2016] to solve Eq. (11). This modeling procedure requires two modules, one for simulating the plate and the other for the fluid.
 116 Each module provides a wide range of equations, which were needed in specifying subdomains and boundaries. For this purpose, some variables are set to make the
 117 connection between these two modules. At fluid-structure interface, kinematic and dynamic continuity has to be ensured. The complete coupled problem has to fulfill
 118 the condition that the location of the fluid-structure interface coincides for both fields. Thus, the fluid-structure interaction boundary condition concerning the fluid
 119 is of a Dirichlet type, and the fluid-structure boundary condition for the solids is given by a Neumann condition. The plate and fluid were simulated using quadratic
 120 element and quadratic Lagrange element, respectively. The plate and fluid elements at the interface shared the same nodes and had extra fine meshes to capture the
 121 details during the coupled vibrations (see Fig. 2). Thus, for the eigenvalue problem solution, which depends on finding the eigenvalues ω , is solved by the natural
 122 frequency extraction.
 123
 124
 125
 126
 127
 128
 129
 130

131 3. Results and discussion

132 This section presents results of the natural frequencies and associated mode shapes of the plate submerged in fluid-filled cylindrical container (Fig. 1). By performing
 133 modal analysis on the plate, first six frequencies are tabulated in Tables 2-4. In order to compare the present results with other established results of specific cases,
 134 we maintain the same frequency factor as the one defined by [Lee *et al.* 2007] in the case of an plate vibrating in vacuum. Thus, in other words, frequencies
 135 are normalized and introduced as the dimensionless frequency, which is defined by $\lambda = a\sqrt{\omega} (\rho_s h / D)^{1/4}$. The geometry and material properties of the plate and the
 136 compressible fluid are presented in Table 1.
 137
 138
 139
 140

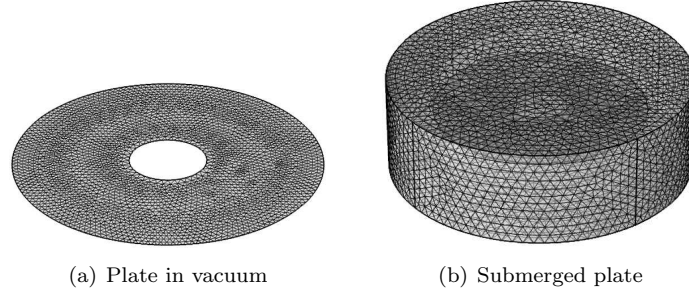


Fig. 2. Plate mesh ($b/a = 0.25$, $a = 0.175$ m). (a) : Mesh consists of 5248 boundary elements and 200 edge elements. Number of degrees of freedom solved for : 64176 and time for solving is 21 s. (b) : Mesh consists of 99865 domain elements, 6784 boundary elements, and 308 edge elements. Number of degrees of freedom solved for : 153770 and time for solving is 151 s.

Table 1. Material and geometrical parameters.

| Properties | Plate and fluid |
|---------------------------|--------------------------|
| Young's modulus, E | 207 (GPa) |
| Density, ρ_s | 7800 (kg/m^3) |
| Poisson's ratio, ν | 0.3 |
| Thickness, h | 0.002 (m) |
| Density, ρ_f | 1000 (kg/m^3) |
| Bulk modulus, B | 2.199 (GPa) |
| Speed of sound, c_f | 1483 (m/s) |
| Radius, R | 0.25 (m) |
| Depth, H | 0.16 (m) |
| Lower region depth, H_l | 0.10 (m) |

141 Tables 2 and 3 show six frequencies using indirect BIEMs method [Lee *et al.*,
 142 2007] and the present FEM. The very good agreement is revealed by showing the
 143 reliability of the implemented algorithm in Comsol Multiphysics code. Table 2 also
 144 shows that the frequency decreases as the plate radius increases. This is related
 145 to the plate mass effect. For the plate with an eccentric hole, Table 3 shows also
 146 that the doublet frequency (multiplicity) divides into two distinct values. This mul-
 147 tiplicity is due to the hole eccentricity. Indeed, the eccentricity generates a local
 148 modification of the mass, hence the doublet frequency [Deutsch *et al.*, 2004]. Figs.
 149 3 and 4 show the mode shapes of the plate with an eccentric hole in vacuum and in
 150 water, respectively. Note that, Fig. 3 is identical to that given by [Lee *et al.*, 2007].
 151 Furthermore, the convergence is very fast to obtain the desirable frequencies. In
 152 addition, the fundamental mode corresponds to the mode with $n = 0$ and $m = 0$.
 153 Thus, in tables 2-4 the parameters n and m define respectively the number of nodal
 154 diameters and nodal circles.

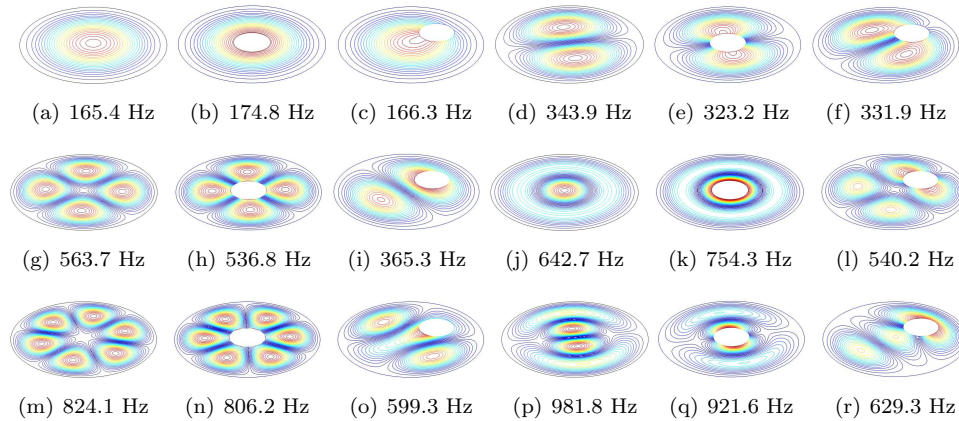
155 In this work, various parameters effects on plate frequencies such hole radius,
 156 hole eccentricity, fluid density and upper fluid height on the coupled frequencies are

Table 2. First six frequencies of the plate in vacuum ($b/a = 0.25$).

| Mode | (n, m) | $a = 0.175$ (m) | | $a = 1$ (m) | | |
|------|----------|-----------------|----------|-------------|-----------|------------------------|
| | | Present | | Present | | Lee <i>et al.</i> 2007 |
| | | f (Hz) | f (Hz) | λ | λ | |
| 1 | (0, 0) | 174.85 | 5.3829 | 3.2743 | 3.2750 | |
| 2 | (1, 0) | 323.25 | 9.9897 | 4.4606 | 4.4610 | |
| 3 | (2, 0) | 536.84 | 16.668 | 5.7618 | 5.7640 | |
| 4 | (0, 1) | 754.34 | 23.3 | 6.8123 | 6.8160 | |
| 5 | (3, 0) | 806.22 | 25.05 | 7.0635 | 7.0680 | |
| 6 | (1, 1) | 921.67 | 28.486 | 7.5323 | 7.5360 | |

Table 3. First six frequencies in vacuum ($b/a = 0.25$, $e = 0.45$ m). * multiplicity.

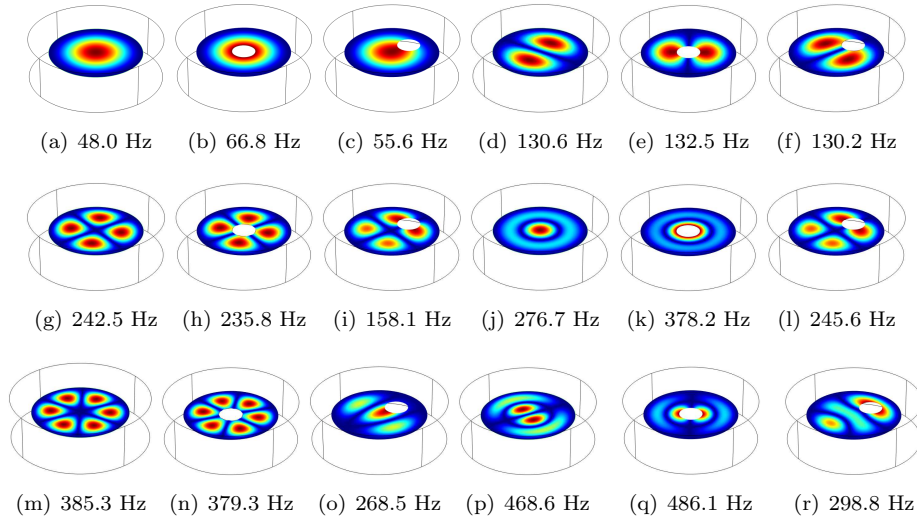
| Mode | (n, m) | $a = 0.175$ (m) | | $a = 1$ (m) | | |
|------|----------|-----------------|----------|-------------|-----------|------------------------|
| | | Present | | Present | | Lee <i>et al.</i> 2007 |
| | | f (Hz) | f (Hz) | λ | λ | |
| 1 | (0, 0) | 166.32 | 5.1448 | 3.2011 | 3.1870 | |
| 2 | (1, 0)* | 331.96 | 10.29 | 4.5271 | 4.5210 | |
| 3 | (1, 0)* | 365.31 | 11.292 | 4.7424 | 4.7400 | |
| 4 | (2, 0)* | 540.21 | 16.721 | 5.7709 | 5.7580 | |
| 5 | (2, 0)* | 599.37 | 18.576 | 6.0826 | 6.0600 | |
| 6 | (0, 1) | 629.36 | 19.485 | 6.2296 | 6.2560 | |

Fig. 3. First six mode shapes of plate in vacuum. (a,d,g,j,m,p) Without a hole ($a = 0.175$ m). (b,e,h,k,n,q) With a concentric hole ($b/a = 0.25$). (c,f,i,l,o,r) With an eccentric hole ($e = 0.45$ m).

157 presented. Firstly, one investigates how hole radius affects the frequencies of plate.
 158 Variation of first ten plate modes is exhibited in Fig. 5(a) for different values of the
 159 aspect ratio b/a of the plate. As the hole radius of the plate increases, the frequencies

Table 4. Six frequencies of plate with a hole in fluid ($b/a = 0.25$, $a = 0.175$ m).

| Mode | $e = 0$ | | $e = 0.45$ (m) | | $e = 0.6$ (m) | |
|------|----------|----------|----------------|----------|---------------|----------|
| | (n, m) | f (Hz) | (n, m) | f (Hz) | (n, m) | f (Hz) |
| 1 | (0, 0) | 66.824 | (0, 0) | 55.605 | (0, 0) | 51.913 |
| 2 | (1, 0) | 132.55 | (1, 0)* | 130.25 | (1, 0)* | 129.89 |
| 3 | (2, 0) | 235.81 | (1, 0)* | 158.19 | (1, 0)* | 147.38 |
| 4 | (0, 1) | 378.29 | (2, 0)* | 245.64 | (2, 0)* | 244.49 |
| 5 | (3, 0) | 379.38 | (2, 0)* | 268.56 | (2, 0)* | 260.00 |
| 6 | (1, 1) | 486.11 | (0, 1) | 298.89 | (0, 1) | 301.88 |

Fig. 4. First six mode shapes of plate in fluid. (a,d,g,j,m,p) Without a hole ($a = 0.175$ m). (b,e,h,k,n,q) With a concentric hole ($b/a = 0.25$). (c,f,i,l,o,r) With an eccentric hole ($e = 0.45$ m).

160 for asymmetric modes ($n > 0$) with $m = 0$ are slightly affected. However, the
 161 frequencies for asymmetric modes with $m \geq 1$ and for axisymmetric modes ($n = 0$)
 162 increase as the hole radius increases. In fact, when the hole radius increases, the
 163 plate effective radius decreases and this causes an increase in the plate stiffness, and
 164 as a consequence the frequencies increase. In addition, in Fig. 5, the intersection of
 165 mode curves with the frequency axis, corresponds to frequencies obtained in case
 166 of an circular plate without hole submerged in fluid. These frequencies are in good
 167 agreement with those obtained by [Askari *et al.*, 2013]. If the plate contains multi-
 168 hole, the context is much more complex. The plate stiffness decreases more than the
 169 mass and therefore the frequencies of a perforated plate are usually smaller than
 170 those of the plate without hole [Lee *et al.*, 2007; Jung and Jeong, 2015]. This is
 171 the opposite situation from that of the plate with a single hole.

172 Secondly, one investigates how the hole eccentricity affects the frequencies. Figs.

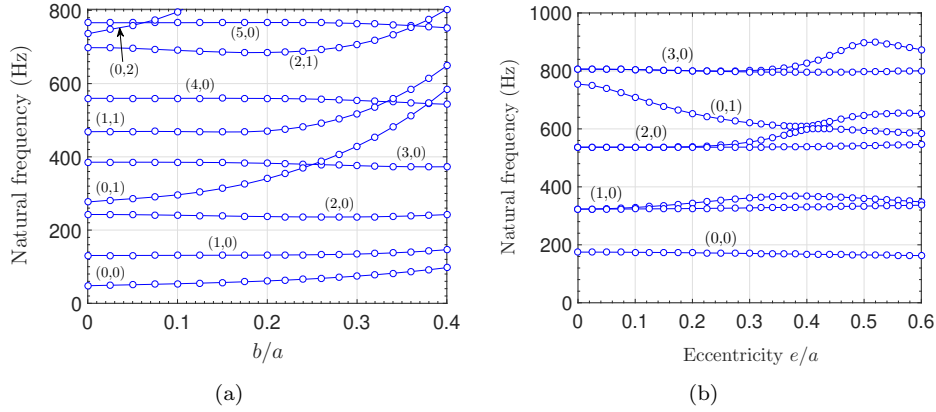


Fig. 5. (a) Radius hole effect on frequencies of submerged plate. (b) Eccentricity effect on frequencies in vacuum ($b/a = 0.25$, $a = 0.175$ m).

173 5(b) and 6(a) show the frequencies in vacuum and in water, varying with the hole
 174 eccentricity. As can be noticed, on the one hand the presence of the fluid around the
 175 plate creates an added mass due to the fluid motion which decreases significantly
 176 the frequencies of the plate. On the other hand Figs. 5(b) and 6(a) show also that an
 177 increase in the eccentricity, leads to an axial symmetry breaking, as a consequence
 178 the doublet frequencies (multiplicity) occurring in the case of plate for asymmetric
 179 modes ($n > 0$), are progressively separated into two distinct values. We can also
 180 observe that for asymmetric modes, the first frequency varies slightly with respect
 181 to the eccentricity. However, with an increase in eccentricity, the second frequency
 182 of the asymmetric modes augments and then decreases beyond a certain eccentricity
 183 value. For example, asymmetric mode (1,0) has the peak frequency at eccentricity
 184 $e/a = 0.37$ in vacuum and in fluid, asymmetric mode (2,0) has the peak frequency at
 185 eccentricity $e/a = 0.42$ in vacuum ($e/a = 0.37$ in fluid), and asymmetric mode (3,0)
 186 has the peak frequency at $e/a = 0.52$ in vacuum ($e/a = 0.5$ in fluid). Therefore,
 187 with the asymmetric modes increasing, the eccentricity where the peak frequency
 188 is obtained increases. In addition, the fundamental mode (0,0) is slightly affected
 189 by increasing in eccentricity. However the axisymmetric mode (0,1) decreases with
 190 increasing eccentricity and increases beyond a certain eccentricity value.

191 Thirdly, to study the fluid density effect (added mass) on the nature frequencies
 192 of the plate, Fig. 6(b) is plotted for first five modes. It is obvious from this figure
 193 that, when the plate vibrates in denser fluid, the frequencies take lower values.

194 Fourthly, one investigates how the frequencies of the plate vary with the upper
 195 fluid height H_u . The frequencies are plotted in Fig. 7(a) as a function of the normal-
 196 ized upper fluid height. When the upper fluid height approaches zero, i.e. the plate
 197 reaches the free fluid surface, the frequencies increase regardless of (n, m), and they
 198 converge to those in the case of the plate in contact with fluid on only one side.
 199 The frequencies decrease continually, but within an interval from 0.2 to 0.8 of the

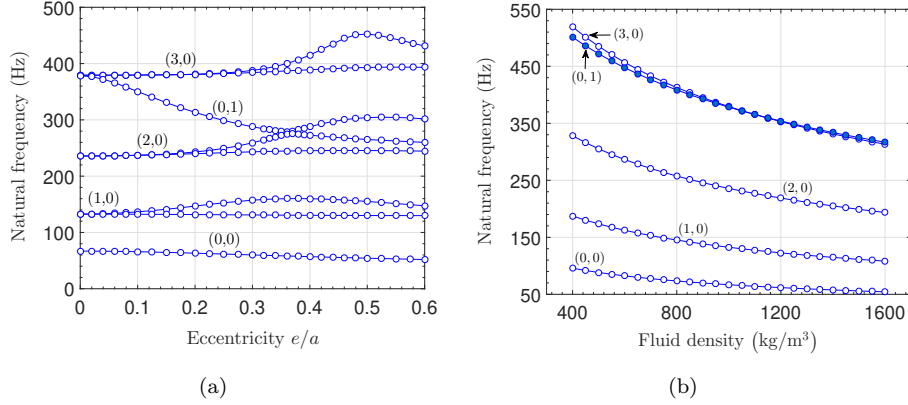


Fig. 6. (a) Eccentricity effect on frequencies in fluid ($b/a = 0.25$, $a = 0.175$ m). (b) Variation of frequencies of plate versus fluid density ($b/a = 0.25$, $a = 0.175$ m).

200 normalized $1 - H_u/H$ fluid height over the plate, they diminish slowly. However,
 201 when the plate approaches the container bottom, the frequencies decrease dramati-
 202 cally due to the increase of the added mass. In addition, when the plate reaches
 203 the free fluid surface, the upper fluid reacts as the in phase mode with respect to
 204 the plate [Ergin and Ugurlu, 2003], mainly the upper fluid moves vertically, and
 205 the added mass of the fluid progressively decreases with decreasing the upper fluid
 206 height. In addition, to study the effects of fluid density and upper fluid height on
 207 the naturel frequencies of the circular plate, Fig. 7(b) is plotted for some values of
 208 fluid density and normalized upper fluid height. It is evident from this figure that,
 209 when the plate is oscillating in contact with the denser fluid, the frequencies takes
 lower values. Note that this behavior is also found for the other modes.

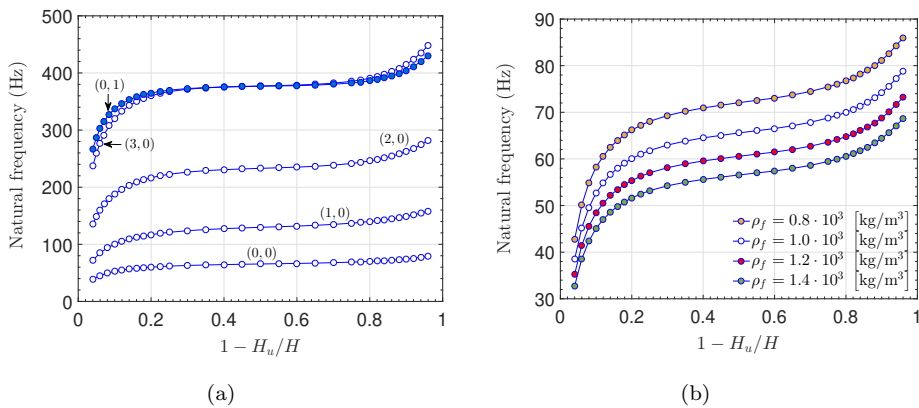


Fig. 7. (a) Frequencies of plate versus normalized upper fluid height in the case of free fluid surface ($b/a = 0.25$, $a = 0.175$ m). (b) Frequencies for the fundamental mode (0,0) of the plate versus normalized upper fluid height in the case of free fluid surface ($b/a = 0.25$, $a = 0.175$ m).

210 Fifthly, to study the case of bounded fluid, the free fluid surface is replaced by
 211 an upper rigid wall. The frequencies are plotted in Figs. 8(a) and 8(b) as a function
 212 of the normalized upper fluid height. The frequencies severely decrease when the
 213 plate approaches the upper rigid surface. In fact, the upper fluid reacts as the out
 214 of phase mode with respect to the plate [Ergin and Ugurlu, 2003], and the upper
 215 fluid moves laterally in the gap between the upper rigid wall and plate, this leads to
 216 an increase in the added mass of the fluid. Fig. 8(a) show also that with the modes
 217 increasing, the difference in the frequencies between the bounded fluid case and free
 218 fluid surface case augments. We can also remark that the frequencies in the free
 219 fluid surface case are always greater than those obtained in the bounded fluid case
 220 when the plate reaches the upper side of the container.

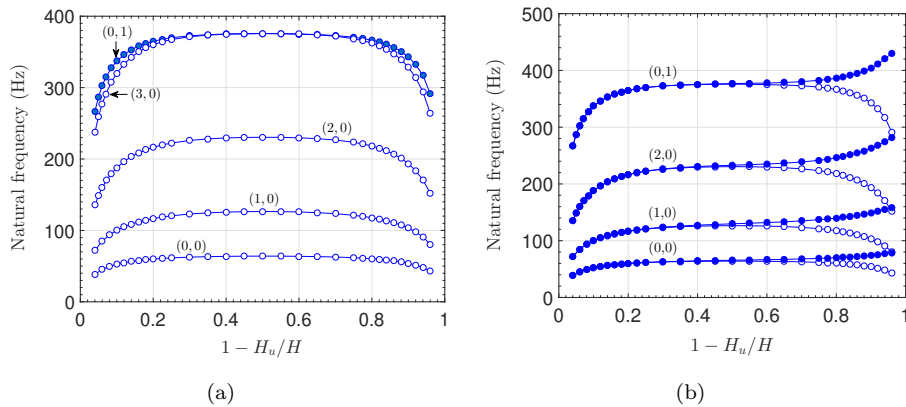


Fig. 8. (a) Frequencies of plate versus normalized upper fluid height for the fluid-bounded case ($b/a = 0.25$, $a = 0.175$ m). (b) Fluid bounding effect on frequencies of plate ($b/a = 0.25$, $a = 0.175$ m). Free fluid surface case (●) and fluid-bounded case (○).

221 Finally, four first sloshing frequencies are plotted in Fig. 9 versus upper fluid
 222 height. it is well known that the submerged plate can be used as a baffle plate to
 223 reduce or suppress the sloshing waves, and simultaneously to decrease the frequen-
 224 cies and change the sloshing mode shapes as shown in two cases. With a decrease
 225 in the normalized upper fluid height, the sloshing frequencies increase. As the plate
 226 approaches the free fluid surface, the sloshing frequencies significantly decrease,
 227 which means that the submerged plate can be used as a baffle device to reduce
 228 or suppress the sloshing waves. In addition, first four sloshing mode shapes of the
 229 free fluid surface are illustrated in Fig. 10 for two different upper fluid heights. The
 230 fluid heights above the plate are equal to $H_u = 4.8$ mm and $H_u = 64$ mm. These
 231 values correspond respectively to a positioning of the plate in the vicinity of the
 232 fluid surface and approximately at the cylindrical container half height. The slosh-
 233 ing modes when the plate is placed at the container bottom are identical to those

234 without plate. Consequently, the positioning of the plate at the container bottom
 235 has no influence on the sloshing modes, whereas the positioning near the free sur-
 236 face greatly reduces the sloshing frequencies. In other words, sloshing frequencies
 237 converge to those without plate once the normalized upper fluid height approaches
 zero as shown in Fig. 10.

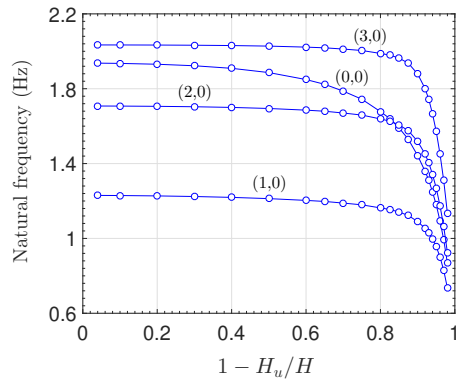


Fig. 9. Sloshing frequencies for the first four modes of plate ($b/a = 0.25$, $a = 0.175$ m).

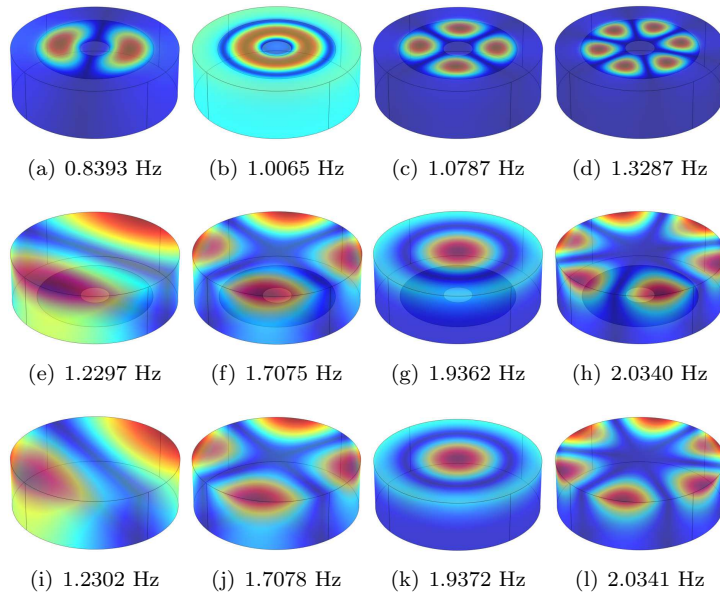


Fig. 10. First four Sloshing mode shapes ($b/a = 0.25$, $a = 0.175$ m). (a,b,c,d) for $1 - H_u/H = 0.97$. (e,f,g,h) for $1 - H_u/H = 0.06$. (i,j,k,l) without plate.

239 4. Conclusion

240 A numerical analysis to investigate the frequencies of a thin circular plate with hole
 241 submerged in fluid is proposed using FEM. The effect of different parameters includ-
 242 ing fluid density, free surface wave, fluid height, hole radius and hole eccentricity
 243 on the frequencies is examined and discussed in detail. The results can serve as
 244 benchmark solutions for the vibration control, parameter identification and damage
 245 detection of thin circular plate with a hole. The following comments were made in
 246 the present study : (i) The results show a good agreement with those in literature
 247 in some particular cases by showing the reliability of the implemented algorithm in
 248 Comsol Multiphysics software and, the convergence is very fast to obtain the desir-
 249 able frequencies. (ii) The hole eccentricity has a slight effect on the first frequency
 250 of asymmetric modes, but the second frequency is strongly affected by the hole ec-
 251 centricity. (iii) When the plate is vibrating in fluid, the frequencies decrease and the
 252 magnitude of the decrease is more important when the fluid density increases. (iv)
 253 The hole radius of the plate affects slightly the frequencies for asymmetric modes
 254 ($n > 0$) with the radial circle $m = 0$. However, the frequencies for asymmetric
 255 modes with the radial circle $m \geq 1$ and for axisymmetric modes ($n = 0$) increase
 256 as the hole radius increases. (v) The frequencies of the plate initially decrease with
 257 the increasing the upper fluid height, then become about constant when the plate
 258 reaches the middle of the container. However, increasing the upper fluid height more
 259 than the container middle height leads to a decrease again in the frequencies, and
 260 this is due to the plate closeness to the container rigid bottom.

261 In addition, the numerical results obtained are in good agreement with existing
 262 data in some particular cases, thereby providing a satisfactory validation of the
 263 present model. In future, the following topics are of interests in order to complete
 264 this article results : (1) The cylindrical container radius effect on the frequencies
 265 may be important in order to know from which critical value of the container radius
 266 the fluid portions far from the plate have a little effect on plate vibration behavior.
 267 (2) In this study, the outer and inner boundaries of the plate are subject to the
 268 clamped and free boundary conditions, respectively. Therefore, it's recommended
 269 to investigate how the plate frequencies vary with different boundary conditions.

270 5. References

- 271 Amabili, M and Kwak, M. K [1996] "Free vibration of circular plates coupled with
 272 liquids: revising the Lamb problem," *J. Fluids Struct.* **10**(7), 743–761.
 273 Askari, E., Jeong, K. H and Amabili, M [2013] "Hydroelastic vibration of circular
 274 plates immersed in a liquid-filled container with free surface," *J. Sound Vib.*
 275 **332**, 3064–3085.
 276 Bahaadini, R and Saidi, A. R [2018] "Stability analysis of thin-walled spinning
 277 reinforced pipes conveying fluid in thermal environment," *Eur. J Mech. A-Solid*

278 **72**, 298–309.

279 Bahaadini, R., Dashtbayazi, M. R., Hosseini, M and Khalili-Parizi, Z [2018a] "Sta-
280 bility analysis of composite thin-walled pipes conveying fluid," *Ocean Eng.* **160**,
281 311–323.

282 Bahaadini, R., Saidi, A. R and Hosseini, M [2018b] "Dynamic stability of fluid-
283 conveying thin-walled rotating pipes reinforced with functionally graded carbon
284 nanotubes," *Acta Mech.* **229**(12), 5013–5029.

285 Bauer, H. F [1995] "Coupled frequencies of a liquid in a circular cylindrical container
286 with elastic liquid surface cover," *J. Sound Vib.* **180**(5), 689–704.

287 Chen, J. T., Lin, S. Y., Chen, I. L. and Lee, Y. T [2006] "Mathematical analysis
288 and numerical study to free vibrations of annular plates using BIEM and BEM,"
289 *Int. J. Numer. Methods Eng.* **65**, 236–263.

290 Cho, D. S., Kim, B. H., Vladimir, N and Choi, T. M [2015] "Natural vibration
291 analysis of rectangular bottom plate structures in contact with fluid," *Ocean*
292 *Eng.* **103**, 171–179.

293 Comsol Multiphysics [2016] "Analysis User's Manual Version 5.2".

294 Deutsch, B. M., Robinson, A. R., Felce, R. J and Moore, T. R [2004] "Nondegenerate
295 normal-mode doublets in vibrating flat circular plates," *Am. J. Phys.* **72**(220).

296 Ergin, A and Ugurlu, B [2003] "Linear vibration analysis of cantilever plates par-
297 tially submerged in fluid," *J. Fluids Struct.* **17**(7), 927–939.

298 Gascon-Pérez, M [2017] "Acoustic influence on the vibration of a cylindrical mem-
299 brane drum filled with a compressible fluid," *Int. J. Appl. Mech.* **9**(5), 1750072.

300 Gascon-Pérez, M and Garcia-Fogeda, P [2015] "Induced damping on vibrating cir-
301 cular plates submerged in still fluid," *Int. J. Appl. Mech.* **7**(6), 1550079.

302 Ghalandari, M., Bornassi, S., Shamshirband, S., Mosavi, M and Chau, K. W [2019]
303 "Investigation of submerged structures' flexibility on sloshing frequency using a
304 boundary element method and finite element analysis," *Eng. Appl. Comp. Fluid*
305 *Mech.* **13**(1), 519–528.

306 Jhung, M. J., Choi, Y. H and Ryu, Y. H [2009] "Free vibration analysis of circular
307 plate with eccentric hole submerged in fluid," *Nucl. Eng. Technol.* **41**(3), 355–
308 364.

309 Jhung, M. J and Jeong, K. H [2015] "Free vibration analysis of perforated plate
310 with square penetration pattern using equivalent material properties," *Nucl.*
311 *Eng. Technol.* **47**(4), 500–511.

312 Jin, H., Liu, Y and Li, H. J. [2014] "Experimental study on sloshing in a tank with
313 an inner horizontal perforated plate," *Ocean Eng.* **82**, 75–84.

314 Khurasia, H. B and Rawtani, S. [1978] "Vibration analysis of circular plates with
315 eccentric hole," *J. Appl. Mech.* **45**(1), 215–217.

316 Kinsler, L. E., Frey, A. R., Coppens, A. B and Sanders, J. V [1999] "Fundamentals

- 317 of Acoustics”, John Wiley & Sons, (1999) New York.
- 318 Kwak, M. K [1991] ”Vibration of circular plates in contact with water,” *J. Appl.*
319 *Mech.* **58**(2), 480–483.
- 320 Lee, W. M., Chen, J. T and Lee, Y. T [2007] ”Free vibration analysis of circular
321 plates with multiple circular holes using indirect BIEMs,” *J. Sound Vib.* **304**,
322 811–830.
- 323 Leissa, A. W and Narita, Y. [1980] ”Natural frequencies of simply supported circular
324 plates,” *J. Sound Vib.* **70**(2), 221–229.
- 325 Mnassri, I and El Baroudi, A [2017] ”Elasto-acoustic coupling between two circular
326 cylinders and dense fluid,” *Int. Appl. Mech.* **9**(5), 24 pages.
- 327 Morand, H and Ohayon, R [1979] ”Substructure variational analysis of the vibra-
328 tions of coupled fluid-structure systems: finite element results,” *Int. J Numer.*
329 *Meth. Eng.* **14**, 741–755.
- 330 Morand, H and Ohayon, R [1995] ”Fluid structure interaction”, John Wiley & Sons.
- 331 Nagaya, K. and Poltorak, K. [1989] ”Method for solving eigenvalue problems of
332 the Helmholtz equation with a circular outer and a number of eccentric circular
333 inner boundaries,” *J. Acoust. Soc. Am.* **85**, 576–581.
- 334 Saidi, A. R., Bahaadini, R and Majidi-Mozafari, K [2019] ”On vibration and stabil-
335 ity analysis of porous plates reinforced by graphene platelets under aerodynam-
336 ical loading,” *Compos. Part B-Eng.* **164**, 778–799.
- 337 Soltani, H and Reddy, J. N [2015] ”Free Vibration Analysis of Elastic Plates in
338 Contact with an Inviscid Fluid Medium,” *Int. J. Appl. Mech.* **7**(3), 1550041.
- 339 Vega, D. A., Vera, S. A., Sanchez, M. D and Laura, P. A. A [1998] ”Transverse
340 vibrations of circular, annular plates with a free inner boundary,” *J. Acoust.*
341 *Soc. Am.* **103**(2), 1225–1226.
- 342 Xue, M. A., Zheng, J., Lin, P and Yuan, X. [2017] ”Experimental study on vertical
343 baffles of different configurations in suppressing sloshing pressure,” *Ocean Eng.*
344 **136**, 178–189.
- 345 Yu, Y. M., Ma, N., Fan, S. M and Gu, X. C [2019] ”Experimental studies of sup-
346 pressing effectiveness on sloshing with two perforated floating plates,” *Int. J*
347 *Nav. Arch. Ocean Eng.* **11**(1), 285–293.